



Citation: Nicoleta Anca Șuțan, Diana Ionela Popescu (Stegarus), Oana Alexandra Drăghiceanu, Carmen Topală, Claudiu Șuțan, Aurelian Denis Negrea, Denisa Ștefania Vîlcoci, Georgiana Cîrstea, Sorin Georgian Moga, Liliana Cristina Soare (2023). *In vitro* cytotoxic activity of phytosynthesized silver nanoparticles using *Clematis vitalba* L. (Ranunculaceae) aqueous decoction. *Caryologia* 76(2): 67-81. doi: 10.36253/caryologia-2330

Received: May 10, 2023

Accepted: October 29, 2023

Published: December 31, 2023

Copyright: ©2023 Nicoleta Anca Șuțan, Diana Ionela Popescu (Stegarus), Oana Alexandra Drăghiceanu, Carmen Topală, Claudiu Șuțan, Aurelian Denis Negrea, Denisa Ștefania Vîlcoci, Georgiana Cîrstea, Sorin Georgian Moga, Liliana Cristina Soare. This is an open access, peer-reviewed article published by Firenze University Press (<http://www.fupress.com/caryologia>) and distributed under the terms of the Creative Commons Attribution License, which permits unrestricted use, distribution, and reproduction in any medium, provided the original author and source are credited.

Data Availability Statement: All relevant data are within the paper and its Supporting Information files.

Competing Interests: The Author(s) declare(s) no conflict of interest.

ORCID

NAȘ: 0000-0001-7459-628X
OAD: 0000-0001-8351-0919
LCS: 0000-0002-2874-3135
DIP: 0000-0002-3442-3760
CT: 0000-0002-9117-4983
CȘ: 0000-0002-1719-1814
ADN: 0000-0001-7525-1056
DȘV: 0000-0002-9777-6782
GC: 0000-0002-7442-7109
SGM: 0000-0001-9620-4283

In vitro cytotoxic activity of phytosynthesized silver nanoparticles using *Clematis vitalba* L. (Ranunculaceae) aqueous decoction

NICOLETA ANCA ȘUȚAN¹, DIANA IONELA POPESCU (STEGARUS)², OANA ALEXANDRA DRĂGHICEANU¹, CARMEN TOPALĂ³, CLAUDIU ȘUȚAN^{3,*}, AURELIAN DENIS NEGREA⁴, DENISA ȘTEFANIA VÎLCOCI⁴, GEORGIANA CÎRSTEA⁴, SORIN GEORGIAN MOGA⁴, LILIANA CRISTINA SOARE¹

¹ Department of Natural Sciences, National University of Science and Technology POLITEHNICA Bucharest, Pitesti University Centre, Romania

² National Research and Development Institute for Cryogenics and Isotopic Technologies-ICSI Ramnicu Valcea, 4th Uzinei Street, 240050 Ramnicu Valcea, Romania

³ Department of Environmental Engineering and Applied Sciences, National University of Science and Technology POLITEHNICA Bucharest, Pitesti University Centre, Romania

⁴ Regional Center of Research and Development for Materials, Processes and Innovative Products Dedicated to the Automotive Industry, National University of Science and Technology POLITEHNICA Bucharest, Pitesti University Centre, Romania

*Corresponding author. E-mail: claudiu.sutan@upb.ro

Abstract. In this study, we report a bottom-up approach for silver nanoparticles (AgNPs) synthesis using aqueous decoction of aerial parts of *Clematis vitalba* L. The phytosynthesized AgNPs were characterized by X-ray diffraction (XRD), UV-vis spectroscopy, Fourier Transform-Infrared Spectroscopy (FTIR), Scanning Electron Microscopy coupled with Energy Dispersive X-ray Spectroscopy (SEM-EDS) and Bright Field Scanning Transmission Electron Microscopy (BFSTEM). The cytogenotoxicity and phytotoxicity assays of AgNPs were assessed by using *Allium* test, Evans blue and 2, 3, 5-triphenyl tetrazolium chloride (TTC) staining, root and stem growth potential, and biomass evaluation. The results revealed that AgNPs were in the size range of 1-15 nm and spherical shape. The biosynthesized AgNPs augment the mitodepressive effect, disruption of cellular metabolism, impairment of root and stem growth, and biomass reduction induced by *C. vitalba* aqueous extracts. These results outline the toxicological profile of the *C. vitalba* extracts, as well as of the phyto-generated AgNPs and provides scientific perspectives on the use of *C. vitalba* extracts as reducing and stabilizing agent for the phytosynthesis of metallic nanoparticles.

Keywords: *Clematis vitalba*, AgNPs, biosynthesis, cytogenotoxicity, phytotoxicity.

INTRODUCTION

Clematis L., one of the best represented genera of the buttercup family (Ranunculaceae), includes about 300 species (He et al. 2019), most climb-

ing plants and shrubs widespread in temperate zones of the northern and southern hemispheres, in mountainous and tropical regions. Over 600 ornamental varieties are commercially cultured worldwide (Weng-Tsai 2003; Woudenberg et al. 2009).

Clematis vitalba L. is a deciduous perennial climber vine which grows in fields and woody areas of Europe, USA, Australia and New Zealand (Bungard 1996; Ogle et al. 2000; Redmond and Stout 2018). In various parts of the world the species *C. vitalba* is known by different common names, such as Old Man's Beard due to its seeds with fluffy heads, Mile-A-Minute based to its high growth rate, or Traveler's Joy, being found along the roads (O'Halloran 2019). Like most buttercups, *C. vitalba* is toxic and irritating, containing protoanemonin lactones and convulsive poisons, but most exposures have resulted in minimal to no toxicity (Duke 1985; Lewis et al. 2020). A synthesis of the compounds identified in *Clematis* species was reported by Da-Cheng (2019), who mentioned the presence of saponin, coumarin, flavonoids, anthocyanins, and alkaloids. In relation to environmental risk, alkaloids and saponins were characterized by Günthardt et al. (2018) as some of the most toxic secondary metabolites. In fact, a large number of papers have shown that buttercups can inhibit mitosis, induce apoptosis and alter the human cell cycle (Naz et al. 2020), but also affect plant cells, being phytotoxic. Thus, the inhibition of root system growth in *Triticum aestivum* L. by ethanolic extracts of *Anemone nemorosa* L. was reported by Ancuceanu et al. (2018). Methanolic extracts from *Anemone reflexa* Steph. & Willd. and *Clematis trichotoma* Nakai showed strong herbicidal activity, inhibiting the growth of barnyardgrass (*Echinochloa crus-galli* (L.) P. Beauv.) seedlings (Kim and Lee 2007).

Phytotoxicity and cytogenotoxicity tests are recommended for assessing the impact of nanoparticles (NPs) on vascular plants. Among the parameters indicated are germination rate, root and stem growth rate, number of leaves, biomass, enzyme activities, photosynthetic rate, mitotic index, i.e. (Roy et al. 2019). The investigation of morphological, physiological and genetic changes in plants under the influence of NPs from natural or anthropogenic sources is still in its infancy (Ogle et al. 2000), from a toxicological perspective the impact proving both positive and negative (RuttikayNedecky et al. 2017).

During the last decades, nanobiotechnology has become an ingenious strategy for green synthesis of NPs. Applying the principle of self-assembly and self-organization through supramolecular interactions and under the action of external stimuli, the bottom-up approach offers the possibility of NPs synthesis in a simple, fast and cost-efficient manner. The use of plant extracts for

extracellular synthesis of NPs is currently an eco-friendly alternative to improve their potential impact, as well as to reduce their side effects (Shende et al. 2022; Şuţan et al. 2016). Along with other metallic nanoparticles, biosynthesized silver nanoparticles (AgNPs) have found their utility in medical, ecological, textile, agriculture, food security and other applications (Eswaran et al. 2021; Hassan and El-latif 2018; Prakash 2013; Roy et al. 2017; Shende et al. 2022). Considered an invasive species (Hill et al. 2001) or potentially invasive (Filippin et al. 2009) in some parts of the world, being so common and having a rapid growth rate, and also being rich in novel secondary metabolites such as flavonoids and alkaloids responsible for the reduction of ionic into nanoparticles, *C. vitalba* could become a valuable resource for the biosynthesis of NPs. Moreover, the biomolecules from the *C. vitalba* could act as capping agents, thus increasing the stability and monodispersity of biosynthesized NPs.

Thus, the aim of this study is to emphasize the potential applicability of the extracts of *C. vitalba* in nanobiotechnology, and their impact, prior to and after AgNPs phytosynthesis on cell viability and metabolic activity, in view of highlighting their cytogenotoxic and phytotoxic properties.

MATERIALS AND METHODS

Collection of plant materials

Overground parts of *C. vitalba* plants were collected from 44°51'23.3"N 24°53'17.7"E (GPSMAP® 60CSx), Piteşti, Romania. The voucher specimen no. 2510 was deposited in the Herbarium of Pitesti University Centre, National University of Science and Technology POLITEHNICA Bucharest, Romania.

Decoction method and synthesis of silver nanoparticles

Authenticated plant material was washed insistently with tap water, rinsed with distilled water and dry until constant weight, at room temperature. The dried plants were ground in pulses for 3 min at 4000 RPM and continuously for 10 sec at 10 000 RPM through a laboratory knife mill (Retsch Knife Mill Grindomix GM 200). The aqueous extract of *C. vitalba* was obtained according to the protocol proposed by Muala et al. (2021) with slight modifications. The powdered raw material was extracted in distilled water (1:10 w/v), in a water bath at 95 °C for 15 min and kept 24 hours at room temperature, in the dark conditions. The slurry was filtered through Wattman No.1 paper to obtain crude extracts.

Aqueous extract of *C. vitalba* (Cv) were treated with equal volume of 10^{-3} M AgNO_3 and left at room temperature. In order to demonstrate the biosynthesis of AgNPs, as well as to correlate the involvement of secondary metabolites from the extract with the biosynthesis process, the extracts were subjected to Fourier Transform-Infrared Spectroscopy (FTIR) analysis and nanoformulations were subjected to X-ray diffraction (XRD), UV-vis spectroscopy, Scanning Electron Microscopy coupled with Energy Dispersive X-ray Spectroscopy (SEM-EDS) and Bright Field Scanning Transmission Electron Microscopy (BFSTEM). The cytogenotoxicity and phytotoxicity assays of extracts and their nanoformulations were assessed by using *Allium* test, Evans blue and 2, 3, 5-triphenyl tetrazolium chloride (TTC) staining.

Physicochemical characterization of C. vitalba aqueous extract and metallic nanoparticles

Aqueous extract was evaluated for its chemical composition. Fourier transform infrared spectroscopy (FTIR) was made with a FTIR Jasco 6300 spectrometer with an ATR accessory equipped with a diamond crystal (Pike Technologies). The spectra were recorded in the region of $4000\text{-}400\text{ cm}^{-1}$, detector TGS, apodization Cosine. The spectral data were processed with JASCO Spectra Manager II software.

AgNPs biosynthesis (CvAg) was evaluated through color change after 4 h and confirmed by UV-Vis spectroscopy.

Qualitative analysis of compounds in Cv (dilution factor 20x) and CvAg was carried out in the wavelength ranging from 300 to 500 nm and the resolution of 2 nm by using UV-Vis Ocean Optics HR2000+. CvAg sample was centrifuged at 6000 rpm for 15 min and the resuspended sediment in a 10 mg/mL solution was scanned for the characteristic peaks (Kaur et al. 2017).

In order to perform X-ray Diffraction Analysis (XRD), the supernatant was removed, and the sediment was centrifuged twice with distilled water at the same speed and time. The XRD pattern of as-separated NPs was recorded with a Rigaku Ultima IV diffractometer. The experimental conditions were: CuK α radiation, BB geometry, D/teX Ultra detector with graphite monochromator, continuously mode, 2theta range $[35^{\circ}\text{-}90^{\circ}]$, step 0.05° , and speed $2^{\circ}/\text{min}$.

Scanning Electron Microscopy coupled with Energy Dispersive X-ray Spectroscopy (SEM-EDS) and Bright Field Scanning Transmission Electron Microscopy (BFSTEM) analyses were performed using the FESEM - HITACHI SU8230 microscope. SEM-EDS was used to confirm the presence of Ag, while STEM was

used to investigate particles shape and size distribution. For SEM-EDS, samples of Cv and CvAg were homogenized in the ultrasonic bath (Guyson's Kerry Pulsatron KC2) for 1 min, dropped on the conductive carbon tape (C) and dried for 24 h in the desiccators. In order to enhance the fluorescence data, a sediment sample obtained by CvAg centrifugation was spread on the conductive carbon tape. EDS data have been collected from the conductive carbon tape (in order to extract sample's support contribution from the EDS spectra), from the Cv, CvAg and CvAg sediment. For BFSTEM analysis, CvAg sample was homogenized in the ultrasonic bath for 1 min, dropped on carbon coated nickel STEM grid (Ni-C) and dried for 24 h in the desiccator. Size distribution of biosynthesized AgNPs was analyzed with ImageJ software (Rasband 1997-2018).

Evaluation of cytogenotoxic effects by Allium test

Healthy bulbs of *Allium cepa* L. (2n=16) were provided by a private organic farm. Bulbs with a diameter of about 3 cm were used for cytogenotoxic assessment. The bulbs were incubated with the discoidal stem in contact with distilled water for 48 hours, in the dark, at room temperature (20-22 °C). The bulbs with new roots were transferred for 12, 24 and 48 h in aqueous extracts of *C. vitalba* (Cv12, Cv24 and Cv24) and nanostructured mixture with AgNPs, respectively (CvAg12, CvAg24, CvAg48). Distilled water (C) was used as a negative control and the cytogenotoxic effects were evaluated at appropriate times of 12, 24 and 48 h (C12, C24, C48) of incubation. Microscopic slides were prepared following the protocol exhaustively previous presented (Sutan et al. 2019). About 3000 cells for each sample were evaluated. Mitotic index (MI), distribution of mitosis phases, chromosomal aberrations and nuclear abnormalities in the analyzed cell population were the endpoints of the cytogenotoxic assessment (Şuğan et al. 2020).

Evaluation of cell viability

Cell viability was assessed by performing Evan's blue test, following the protocol proposed by Vijayaraghavareddy et al. (2017) with slight modifications. After the completion of the experimental treatments, 10 freshly harvested roots corresponding to each experimental variant were incubated for 15 min in 2 ml of 0.25% Evan's blue. The roots were rinsed insistently with distilled water and kept in fresh distilled water overnight. Root tips of 5 mm in length were transferred to 2 ml of 1% aqueous SDS solution and kept for 1 h at 50 °C in

water bath. The roots were qualitatively analyzed and the Evan's blue uptake was macro-imaged. For a quantitative estimation of cell viability, the optical density (OD) of the released pigment was read by the spectrophotometer (UV-Vis, T70+) at 600 nm.

Evaluation of mitochondrial activity

The 2,3,5-triphenyl tetrazolium chloride (TTC) staining assay was applied for assessing the metabolic activity of root tip cells. The onion roots were immersed in 0.5% aqueous TTC solution overnight and then extracted into 3 ml of 95% ethanol for 5-15 min, without heating. Due to the instability of TTC to light, the assay was performed in the dark. The absorbance of the extracts was read at 485 nm with a T70 + UV-Vis spectrophotometer (Towill and Mazur 1974; Prajitha and Thoppil 2017).

Assessment of the phytotoxic effect

Phytotoxicity of aqueous extracts and nanostructured mixture were assessed using seeds of *Triticum aestivum* L., Miranda variety. The seeds were soaked in 150 ml distilled water for 2 h. For each experimental variant 10 imbibed seeds were transferred in *C. vitalba* extract with and without phytothesized AgNPs for one hour, in the dark, and watered periodically with distilled water. Distilled water was used as negative control. After 4 days, fresh and dry biomass, the length of the roots and stems were evaluated. In order to establish dry biomass, the fresh materials were kept in the oven, at 80 °C, until constant weight was obtained (Azooz et al. 2012).

Statistical interpretation

Three replicates were used to quantify the cytogenotoxic and phytotoxic effects of the extracts and nanostructured mixtures. Statistical analysis of the results was performed using IBM SPSS Statistics 20.0 (2011). Statistical significance and significant differences between variables were determined using variance analysis (One Way ANOVA) and the Duncan test for multiple comparisons, respectively. The values of $P \leq 0.05$ were considered statistically significant. Graphs and tables were compiled based on mean values \pm standard error (SE) of several independent experiments. For linear association between variables, Pearson's correlation was significant at the 0.01 level (2-tailed).

RESULTS

Physicochemical characterization of C. vitalba extract prior to and after AgNPs phytosynthesis

The FTIR analysis revealed the band at 3347 cm^{-1} which intensity has almost reduced and shifted to 3359 cm^{-1} in IR spectra of AgNPs. In the case of AgNPs the peaks at 1267 cm^{-1} and at 1046 cm^{-1} are shifted. The strong band at 1636 cm^{-1} existing in the spectrum of *C. vitalba* aqueous extract, are shifted in the FTIR spectrum of the AgNPs as it is shown in Figure 1.

Figure 2 shows a typical metallic Ag XRD pattern, according to ICDD PDF4+ DB04-002-1347. The crystallite size of AgNPs was calculated using Rigaku PDXL2 and Wagner-Halder method (Halder and Wagner, 1966). The obtained value was 10.7 ± 0.4 nm. Furthermore, the biosynthesis of AgNPs was indicated by the visible color shift from greenish-brown to light brown after 2 hours of incubation in the dark, without stirring the mixture (Fig. 3).

The UV-vis spectra of aqueous extracts of *C. vitalba* (Fig. 4A) showed a shoulder peak in the range of 320-330, while the UV-vis spectra of CvAg sample showed a distribution of peaks varying between 400-500 nm, with maximum absorbance at 436 nm (Fig. 4B).

EDS analysis was performed to confirm the presence of Ag. The EDS spectra obtained for the conductive carbon tape, Cv, CvAg and CvAg sedimented on the carbon grid are shown in figure 5. Comparison of the obtained EDS spectra revealed that the aqueous extract of *C. vitalba* contains as majority elements K, Ca, Cl and minority elements such as P, Br, Mg. From analysis of all the superimposed spectra, the presence of Ag can be noticed only in the samples CvAg and CvAg sedimented. Moreover, the EDS pattern did not show any evidence for nitrogen.

In Figure 6A-D the dispersion of biosynthesized AgNPs is represented in BFSTEM at successive magnifications (x20k, x100k, x200k and x500k). The size of the identified particles was below 15 nm, and their shape was relatively spherical (Fig. 6D). It should be noted that a microparticle consisting of AgNPs embedded in a complex biological matrix was identified on the edges of the Ni-C grid and an EDS mapping analysis was performed (Fig. 7).

The analysis of the AgNPs size distribution was performed on the micrograph obtained in BFSTEM (Figure 6D). For the selected area of interest and for the inclusion criterion defined for the range 1-15 nm it was found that AgNPs with domains between 1-10 nm are prevalent.

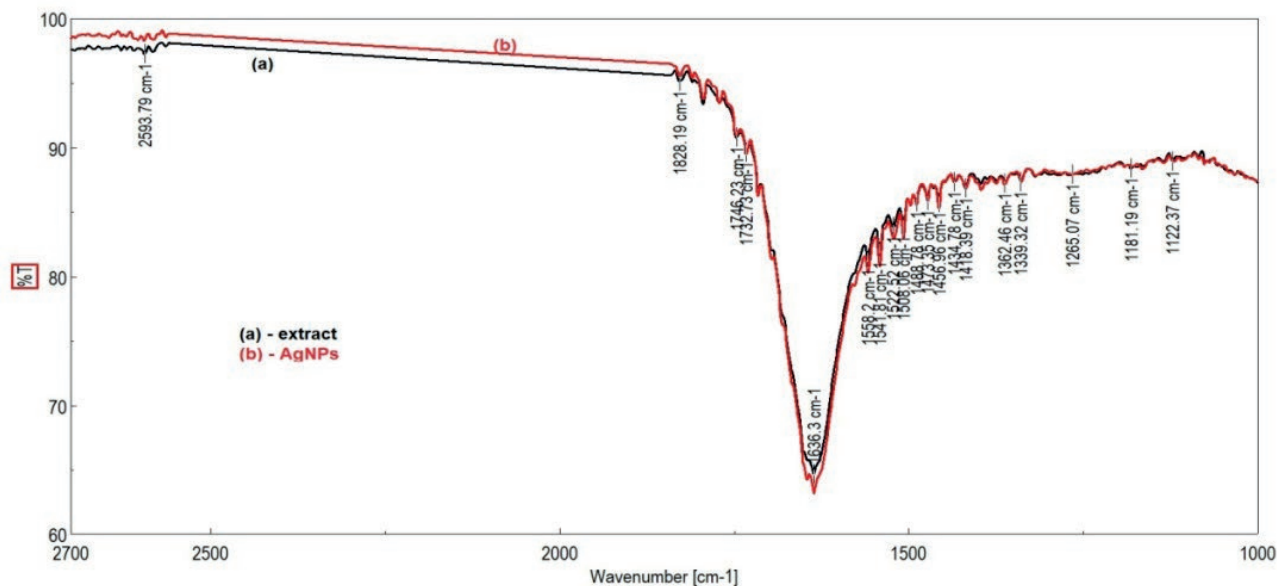


Figure 1. (ATR)-FTIR spectra of *C. vitalba* leaves extract (black) and of AgNPs (red).

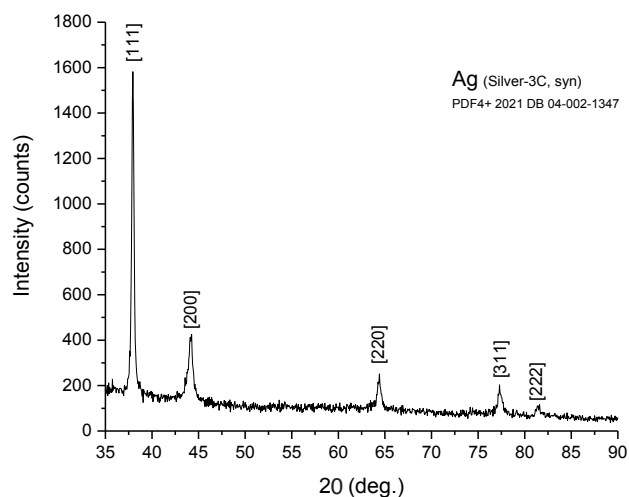


Figure 2. XRD spectra of the phytosynthesized AgNPs using aqueous extract of *C. vitalba*.



Figure 3. Color of *C. vitalba* extract prior (Cv) and after AgNPs phytosynthesis (CvAg).

Cytogenotoxic effects of C. vitalba extract and nanostructured mixture

The effects of *C. vitalba* extracts prior to and after AgNPs biosynthesis on onion meristematic root cells are presented in Table 1. Statistical analysis of the results revealed a significant decrease in MI in the samples defined by aqueous extracts and nanostructured mixtures. The highest MI (8.7%) was recorded for the negative control C12, and the lowest MI (0.6%) was determined in the CvAg48 sample. The Pearson corre-

lation coefficient was -0.87 indicating a significant time dependent inhibition of MI. Nanoformulations with AgNPs determined a severe mitoinhibitory activity, the number of cells identified in the various stages of mitosis being almost zero, after 48 hours from the initiation of treatment.

Suppression of mitosis resulted in a low frequency of chromosomal and nuclear aberrations. However, remarkable differences were noted between the control and the samples defined by *C. vitalba* extracts. Thus, in

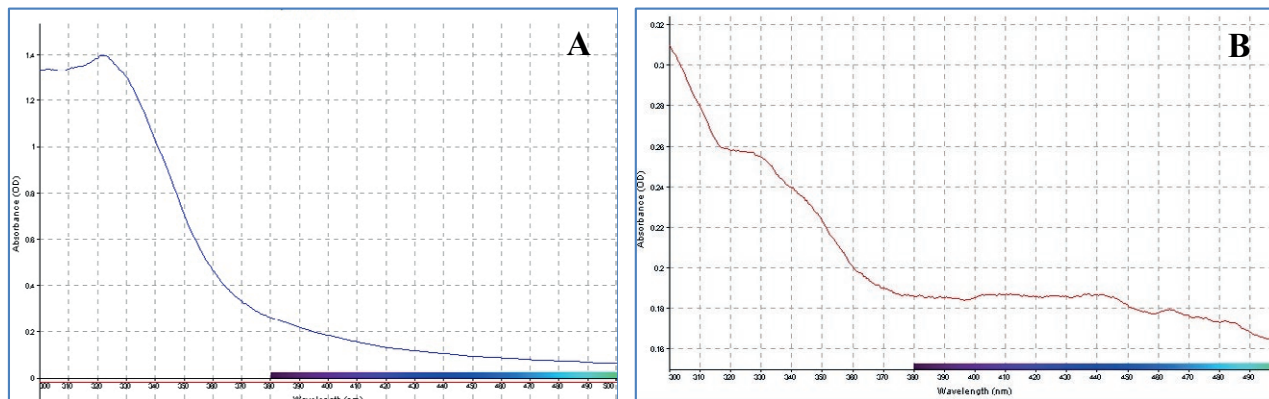


Figure 4. UV-vis spectra of *C. vitalba* prior to (A) and after AgNPs phytosynthesis (B).

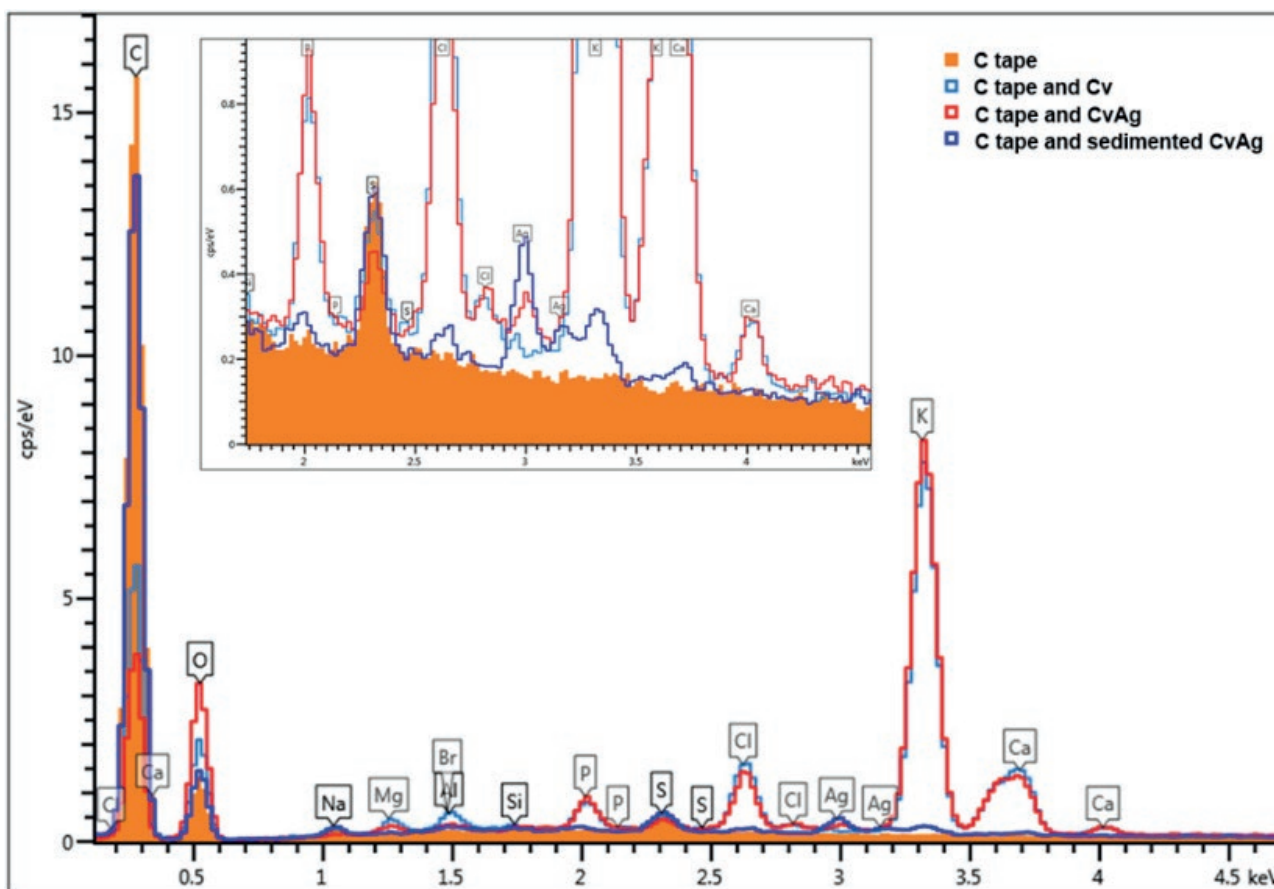


Figure 5. EDS spectra obtained for the conductive carbon tape, Cv, CvAg and CvAg sediment (inset zoom EDS spectra reveal prominent silver peaks).

the control only chromosomal aberrations such as anaphase bridges and very rarely laggards were identified, while *C. vitalba* extracts before and after AgNPs phytosynthesis induced the formation of binucleate and giant

cells with displaced nuclei. Additionally, concave plasmolysis was very often revealed by cytological analysis (Fig. 8).

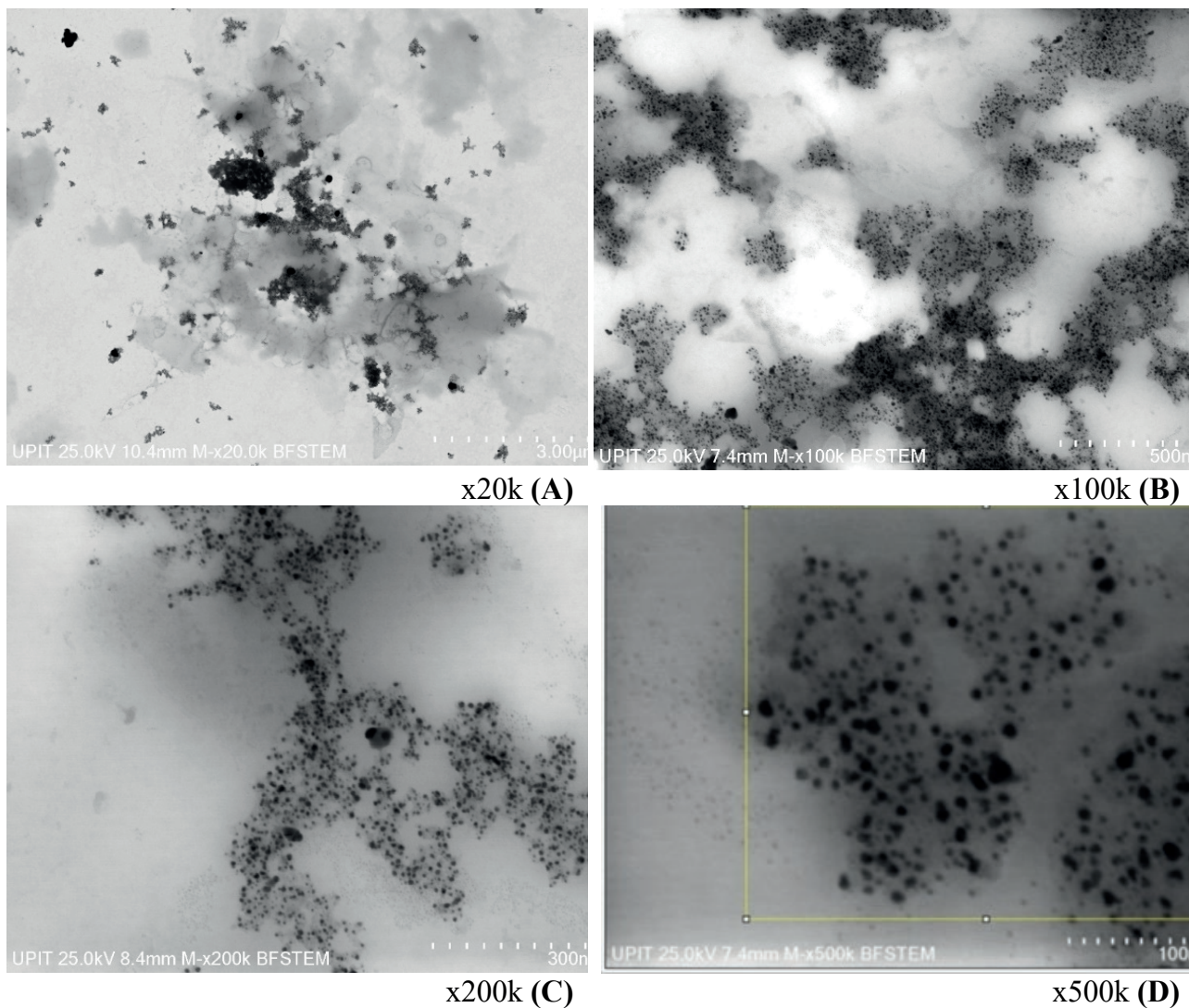


Figure 6. AgNPs dispersion and dimensional analysis on dispersion in BFSTEM.

Evaluation of cell death by Evans blue staining

The permeability of cell membranes in the experimental variants defined by *C. vitalba* aqueous decoction decreased compared to control (Fig. 9). In opposition, incubation of meristematic cells in the CvAg mixture led to an increased uptake of Evans blue, irrespective of treatment duration, suggesting the cytotoxic effect of biosynthesized AgNPs.

Evaluation of viable cells using TTC staining

In Figure 9 is presented the formation of red formazan in meristematic root cells of *A. cepa* and the

formazan absorbance. The data suggests that the reduction of TTC by electrons from the mitochondrial electron transport chain (Towill and Mazur 1975) progressively decreased from negative control to aqueous decoction of *C. vitalba*. The absorbance of formazan increased to 0.68 after 12 h from the start of treatment with AgNPs-supplemented extract and remained low after 48 h of incubation.

Assessment of phytotoxicity on T. aestivum

In the Figure 10 is presented the phytotoxicity of *C. vitalba* extract prior to and after AgNPs biosynthesis. The application of *C. vitalba* extract with and without AgNPs

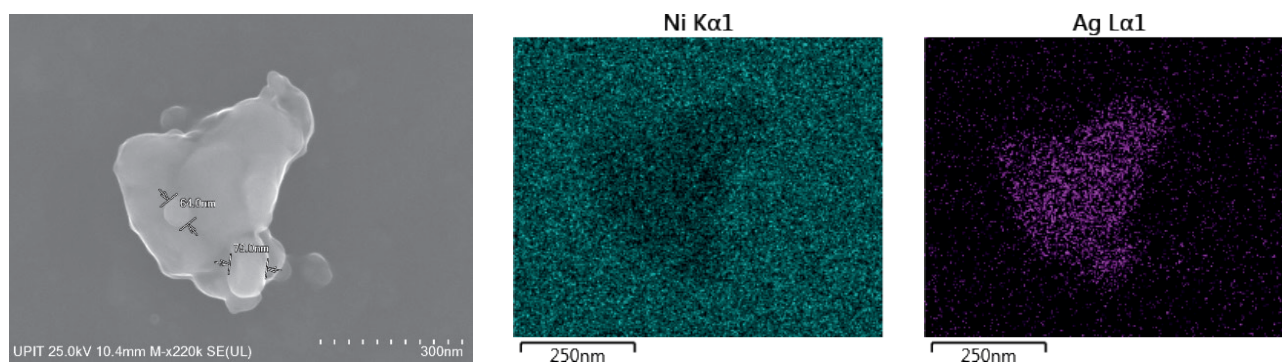


Figure 7. EDS-mapping on the microparticle: Ni grid sample holder (left) and Ag mapping (right).

Table 1. The effects of *C. vitalba* extract and its nanostructured mixture on mitotic index, mitotic cycle and nuclear abnormalities of the *A. cepa* meristematic roots cells (a, b, c, d, e – the interpretation of the significance of the differences by means of the Duncan test, $p < 0.05$).

Experimental variants	MI (%)	Prophase (%)	Metaphase (%)	Anaphase (%)	Telophase (%)	Binucleate cells (%)	Giant cells (%)	Anaphase bridge (%)
C12	8.4±0.7a	35.7±4.4d	27±3.3bc	21.6±3.2a	15.7±0.5abc	0e	0c	15±5.1a
C24	5.5±0.8b	29.2±2.4d	34.6±7ab	18.6±3.4ab	17.7±5.2ab	0.1e	0c	6.7±3.6ab
C48	5.8±1.1b	26.8±5.1d	41.9±1.7a	20±4.6a	11.3±1.4bc	0e	0c	14.8±5.2a
Cv12	2.1±0.1c	62±1.2bc	21.3±1.8c	13.4±1.8abc	3.3±1.6cd	0.2±0.1cd	0c	0b
Cv24	1.7±0.1c	70.9±5.2abc	15.6±1.6c	9.7±1.7bcd	3.8±1.9cd	0.3±0.1bc	0c	0b
Cv48	1.3±0.1c	59.4±6.8c	25.5±4.4bc	8.6±4.8cde	6.5±3.3cd	0.5b	0.1±0.1ab	0b
CvAg12	1.3c	77.8±4.8b	19.6±2.7c	2.6±2.6de	0 d	0.7±0.1a	0.1±0.1ab	0b
CvAg24	1±0.2c	82.2±6.7a	15.2±4.3c	2.6±2.6de	0 d	0.2cd	0.2±0.1a	0b
CvAg48	0.6c	77.8±5.6b	22.2±5.6bc	0e	0 d	0.1±0.1de	0.2±0.1a	0b

on *T. aestivum* seeds had a stimulatory effect on root and stem elongation, and fresh weight compared to control, without significant differences between these variants. The dry biomass of wheat seeds was significantly reduced by AgNPs when compared with negative control.

DISCUSSION

Physicochemical characterization of C. vitalba extract and its nanoformulations

The band at 3347 cm^{-1} revealed by the FTIR analysis corresponded to the -OH groups of phenolic compounds and -NH stretching of the proteins (Borchert et al. 2005; Prakash et al. 2013). The reduced intensity and shifting in IR to 3359 cm^{-1} spectrum of AgNPs indicated the involvement of -OH group in the biosynthesis of AgNPs (Kumar et al. 2016). Similarly, the band at 1636 cm^{-1} revealed for Cv sample was shifted in the FTIR spectrum of the AgNPs, inferring that the -OH group

of the phenolic compounds and carboxylate groups of the extract might have bond to silver ions. At the same time, shifting and decreasing bands intensity of peaks 1267 cm^{-1} and at 1046 cm^{-1} found for the sample CvAg are related to the C-O linkages or C=O stretching from phenolic and ceto compounds (Fig. 1).

After 2 hours of incubation in the dark, at room temperature, the reaction mixture changed from greenish-brown to light brown (Fig. 3). The color change of the reaction solution has often been mentioned as a marker of successful AgNPs biosynthesis (Chhatre et al. 2012; Şuţan et al. 2016; Reddy et al. 2021; Lalsangpuii et al. 2022).

The shoulder peak in the range of 320-330 of the UV-Vis spectra of Cv sample (Figure 4), suggests the presence of flavonoids as a major phenolic compound of aqueous decoction of *C. vitalba* (Arabshahi-Delouee and Urooj 2007). These results are in accordance with the method of preparing extracts, knowing that hot water is used for the extraction of phenols and flavonoids (Valencia-Avilés et al. 2018). The maximum absorbance

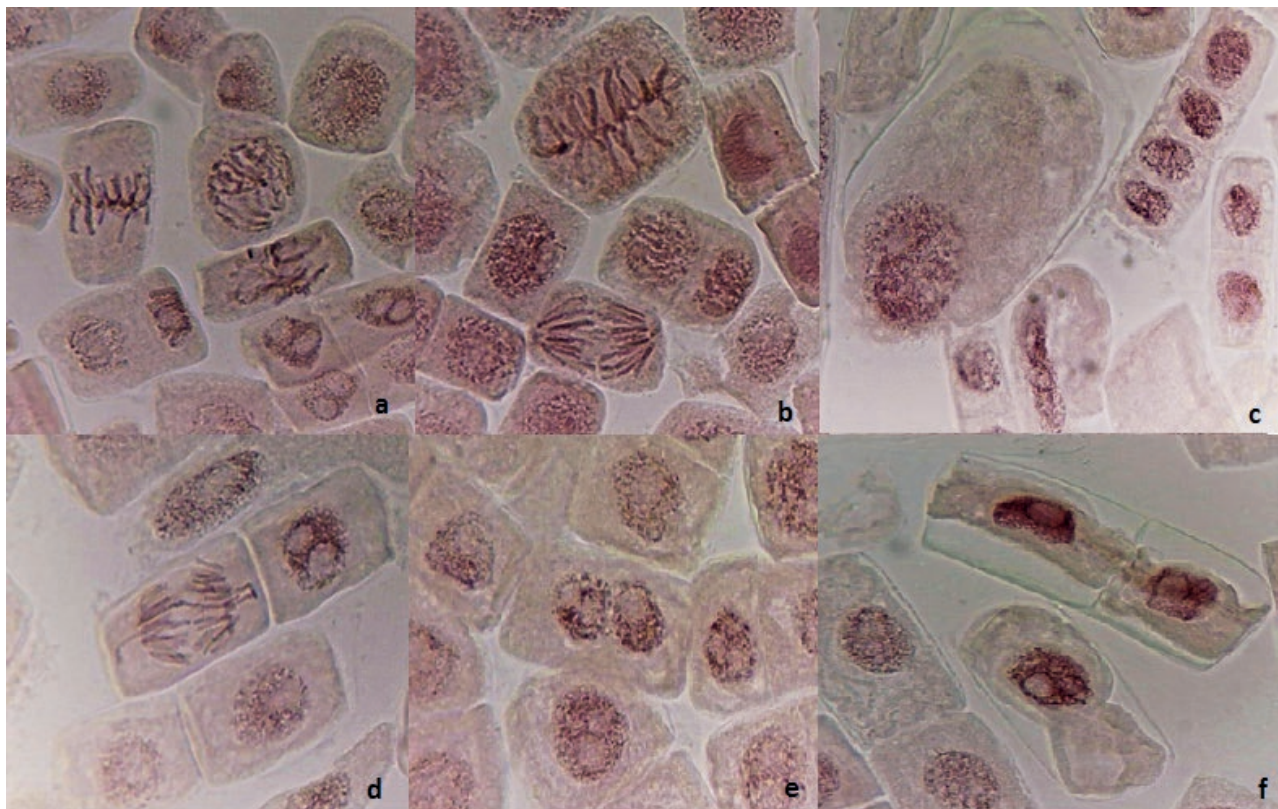


Figure 8. Mitosis, chromosomal aberrations and nuclear abnormalities observed in the root cells of *A. cepa* L. treated with *C. vitalba* L. extracts. (a) - normal prophase, metaphase and telophase (C); (b) - normal metaphase and anaphase (C); (c) - giant cells (CvAg24); (d) - anaphase bridge and laggards (C); (e) - binucleate cell (Cv12); (f) - plasmolysis (Cv48).

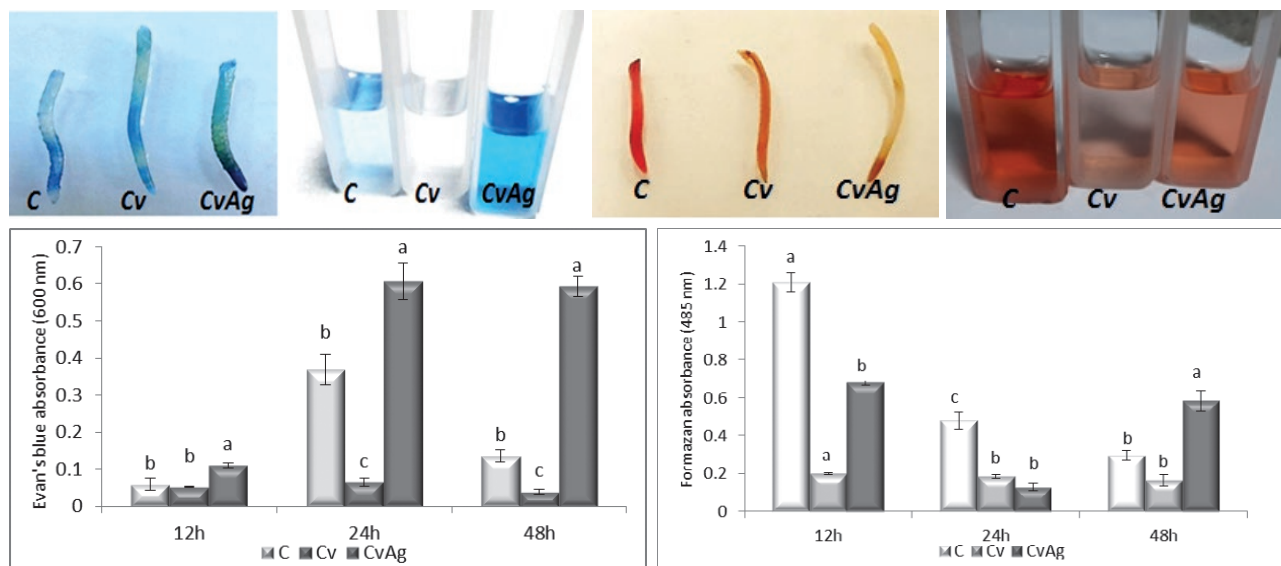


Figure 9. Variation of *A. cepa* meristematic root cell death (left) and root cell viability (right) after treatment with *C. vitalba* aqueous extracts prior to and after AgNPs biosynthesis (a, b, c - the interpretation of the significance of the differences by means of the Duncan test, $p < 0.05$).

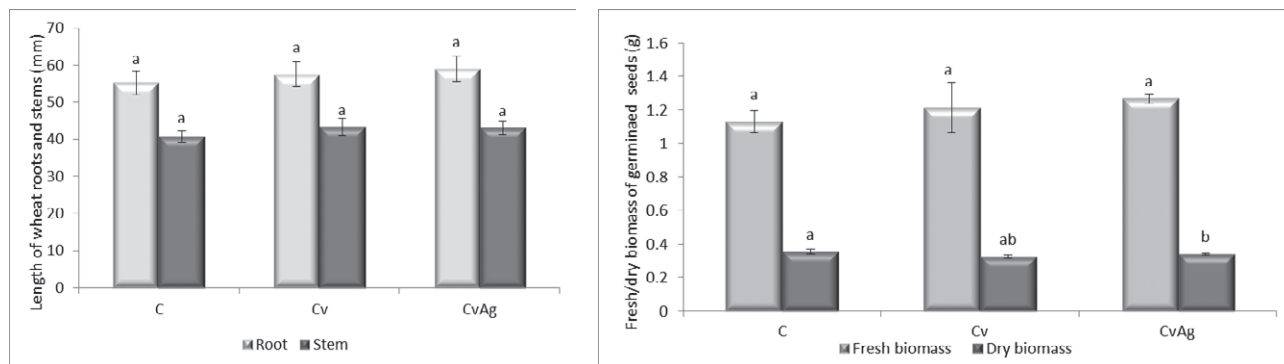


Figure 10. The phytotoxicity of *C. vitalba* extract and its nanostructured mixture on *T. aestivum* seeds: (A) root and stem growth (B) dry and fresh biomass of germinated seeds (a, b, c – the interpretation of the significance of the differences by means of the Duncan test, $p < 0.05$).

at 436 nm characteristic for CvAg sample (Fig. 4B) is an indicator of the presence of AgNPs. The data in the literature suggest that the presence of peaks closer to the wavelength of 400 nm are characteristic of NPs with dimensions of about 10 nm (Martínez-Castañón et al. 2008). Moreover, the position of the peaks specific to AgNPs is also influenced by the shape of the particles, the interaction between them, as well as the density of free electrons and the dispersion medium (Desai et al. 2012; Agnihotri et al. 2014). The data obtained are consistent with the established literature, polyphenols being frequently considered as reducing agents of silver ions (Tyagi et al. 2021).

Some authors appreciate that the absence of ions from AgNO_3 initially added to the extract is an indication of their reduction and of the successful AgNPs synthesis (Kambale et al. 2020; Kthiri et al. 2021).

The observed microparticle embedded in a complex biological matrix may be due to the agglomeration of several AgNPs (Taurozzi et al. 2011). The identification of these microparticles suggests the action of secondary metabolites as capping agents for AgNPs (Kambale et al. 2020). A stabilized coating of biosynthesized AgNPs using plant extracts were previously noticed (Jacob et al. 2019). The high free energy from the surface of NPs causes the selective and progressive adsorption of biomolecules on their surface when they come in contact with complex biological liquids (Monopoli et al. 2012). The composition of this biomolecular capping depends on the size, charge, shape of NPs, on the nature of the biological fluids in which NPs are dispersed, hydrophobicity of NPs surface and surface roughness (Piloni et al. 2019; Marichal et al. 2020). Thus, NPs acquire an identity, which must be taken into account in assessing their biological fates and functions (Wypij et al. 2021).

Cytotoxicity, genotoxicity and phytotoxicity of C. vitalba extracts prior to and after AgNPs biosynthesis

The *Allium* test was proposed as a standardized method in environmental monitoring, being a fast, low-cost, sensitive test and having a good correlation with other test systems (Fiskesjö 1985). *A. cepa* is a genetic model frequently used to evaluate the cytogenotoxicity (mitotic index, chromosomal and nuclear abnormalities) and mutagenicity (micronucleus) of chemicals and their mechanism of action on the mitotic apparatus, allowing the detection of clastogenic and/or aneugenic effects (Wieczerszak et al. 2016; Bonciu et al. 2018).

In our study, the severe inhibition of mitosis can be attributed to the application of the treatment with the whole and undiluted extract of *C. vitalba*, suggesting a high toxicity on onion meristematic cells, even only after 12h. The bioactive compounds of the buttercup family, most of them secondary metabolites, induce cell cycle arrest, apoptosis, and inhibit cell proliferation (Segneanu et al. 2015; Hao et al. 2017). Triterpenoid, saponins, phenolic acids have been mentioned by Łaska et al. (2021) as potent suppressors of HeLa cells growth and proliferation. It has been suggested that active protoanemonin, released by splitting the glycoside ranunculin, can alkylate proteins and DNA (Wink 2010).

Treatment with *C. vitalba* extract and its nanoformulation inhibited mitosis in onion root tips, blocking cells in prophase and significantly reducing the frequency of other phases of mitosis, in a time-dependent manner (Table 1). It is important to note that after 48 hours of incubation in CvAg48, the frequency of anaphase and telophase was zero. These results may be attributed either to suppressing DNA synthesis preventing the cells entering mitosis or to alteration of prophase and prometaphase stages (El-Ghamery et al. 2000). These results confirm the severe cytotoxic effects of the tested extracts and nanoformulations on meristematic

root cells of *A. cepa*. Recent studies showed the specificity of AgNPs towards ds DNA, to which it binds and determines its destabilization (Pramanik et al. 2016).

Giant cells may be polyploid formed by endomitosis or endoreduplication (Bonciu et al. 2018) or may suggest altered signals for cell growth (Hammann et al. 2020). The cause of binucleate cell formation may be due to inhibition of cytokinesis after telophase (Nefic et al. 2013) or cell plate formation (De Keijzer et al. 2014). However, both types of mitotic abnormalities suggest a disruption of the functioning of the microtubules that make up the mitotic spindle and cell plate, on the basis of which *C. vitalba* decoct can be classified as aneugenic agent.

It has been proved that during plasmolytic process, cortical microtubules and actin microfilaments are subjected to architectural changes depending on the severity of water flow (Lang et al. 2014). Microtubules and actin filaments play important roles in establishing the division plan by forming the preprophase band and by forming the phragmoplast that directs the vesicles to form a new cell wall (Rasmussen et al. 2013). Other studies revealed that some substances allow cell plate initiation, but is ultimately disintegrated and the phragmoplast microtubules break down (Valster and Hepler 1997). Disrupting the organization of these structures may be the cause of nuclear aberrations and mitotic inhibition.

Evans blue staining was applied to assess cell membrane integrity. Damaged cell membranes are unable to exclude dye and cells are stained blue. Based on the direct correlation between extracted Evans blue optical density and cell membrane damage, Evans blue staining is a method used to evaluate the cytotoxicity of external stimuli (Roy et al. 2019).

Geisler-Lee et al. (2013, 2014) found that AgNPs were progressively accumulated in root cells. Following this bioaccumulation, severe cytotoxicity may be due to AgNPs coating developed during the bottom-up approach of their biosynthesis. It has been suggested that coating of AgNPs affects cellular responses and alters cell fate (Riaz Ahmed et al. 2017). Cytotoxicity caused by biosynthesized AgNPs in broth of *Pandanus odorifer* (Forssk.) Kuntze (Panda et al. 2011) or by citrate-stabilized AgNPs were previously mentioned (Gorczyca et al. 2022).

In contrast to the Evans test, TTC is used to assess cell viability. TTC is reduced by the mitochondrial dehydrogenase (active only in the living cells) to red formazan. Therefore, formazan stains only the viable cells and the optical density of the extracted formazan decrease in damaged cells (Roy et al. 2019).

The amount of formazan produced directly relates to mitochondrial electron activity, and is proportional to the amount of oxidative damage. In our study, the

results suggest high enzymatic activity following stress (Towill and Mazur 1975) imposed by AgNPs and reduced oxidative damage of respiratory processes, perhaps due to adaptive tolerance capacity (De Ronde and van der Mescht 1997). Furthermore, a non-enzymatic reduction of TTC may have been generated under the conditions of incubating onion roots in CvAg, such as incubation time, temperature and pH (Burdock et al. 2011).

Nanoparticle-induced phytotoxicity can be assessed by morphophysiological (germination rate, root/stem growth potential, biomass, transpiration rate, chlorophyll content, water absorption capacity, etc.), cellular or molecular changes (Yan and Chen 2019; Heikal and Şuţan 2021).

In our study, improving the growth of roots and stems, but also fresh biomass compared with control may be due to the process of overcompensation hormesis, which is an adaptive response to disruption of homeostasis induced by low levels of stress (Calabrese and Baldwin 2002). Testing the phytotoxicity of different concentrations of uncoated AgNPs with an average size of 13.8 ± 2.5 nm on vegetative growth stages of *T. aestivum*, Cui et al. (2014) reported similar results. The mode of interaction and cytogenotoxic effects of NPs depend on many factors, such as the path of synthesis, concentration, exposure time, species, growth stage, etc. (Cui et al. 2014; Heikal and Şuţan 2021). The particularities of biosynthesized metallic nanoparticles can significantly influence their biological effects. Their cytogenotoxic action depends on numerous factors, such as dosage and exposure duration but also on their chemical composition, surface properties, size and shape. The biosynthesized AgNPs triggered various toxic effects (inhibition of mitosis, disruption of cellular metabolism, impairment of root and stem growth and biomass) that could be attributed to numerous factors, such as dosage and exposure duration but also on their chemical composition, surface properties, size and shape (Heikal and Şuţan, 2021). Furthermore, the presence of a surface coating based on the premise that biosynthesized NPs in *C. vitalba* extracts presents various capping biomolecules that influence their morphology, size and stability, which leads to the diversification of bio-nano interactions. Thus, further studies comparing the phytotoxicity of NPs with and without surface coating, as well as identification the secondary metabolites bound on their surface and the way of modulating their own bioactivity, should be performed.

CONCLUSIONS

The bottom-up approach of AgNPs biosynthesis was successfully performed using *C. vitalba* aqueous decoc-

tion, which proved to be rich in polyphenols. Phytosynthesized AgNPs had approximately spherical shape, sizes ranging from 1-15 nm. The formation of a biomolecular capping induced changes in the size of the green synthesized AgNPs. Severe mitoinhibitory effects of *C. vitalba* extracts were amplified after phytosynthesis of AgNPs. The biosynthesized AgNPs manifested cytogenotoxicity and phytotoxicity by mitosis suppression, disruption of cellular metabolism, impairment of root and stem growth and biomass. Further studies are required to determine the mechanism of coated and uncoated AgNPs and the effects of coat-type of biosynthesized metallic nanoparticles.

FUNDING

This work was supported by a grant of the Romanian Ministry of Research, Innovation and Digitization, CNCS-UEFISCDI, project number PN-III-P4-ID-PCE-2020-0620, within PNCDI III.

REFERENCES

- Agnihotri S, Mukherji S, Mukherji S. 2014. Size-controlled silver nanoparticles synthesized over the range 5–100 nm using the same protocol and their antibacterial efficacy. *RSC Adv.* 4:3974–3983. doi: 10.1039/C3RA44507K.
- Ancuceanu R, Căplănuşi R, Anghel IA, Stoicescu CS, Hovaneţ MV, Dinu M. 2018. Assessment of *Anemone nemorosa* L. toxicity. *Acta Med Marisimensis*, 64 Supplement 3:7-7.1/2.
- Arabshahi-Delouee S, Urooj A. 2007. Application of phenolic extracts from selected plants in fruit juice. *Int J Food Prop.* 10:479-488. doi: 10.1080/10942910600891279.
- Azooz MM, Abou-Elhamd MF, Al-Fredan MA. 2012. Biphasic effect of copper on growth, proline, lipid peroxidation and antioxidant enzyme activities of wheat (*Triticum aestivum* cv. Hasaawi) at early growing stage. *Aust J Crop Sci.* 6:688–694.
- Bonciu E, Firbas P, Fontanetti CS, Wusheng J, Karaismailoğlu MC, Liu D, Menicucci F, Pesnya DS, Popescu A, Romanovsky AV, et al. 2018. An evaluation for the standardization of the *Allium cepa* test as cytotoxicity and genotoxicity assay. *Caryologia* 71(3):191–209. doi: 10.4236/ajps.2020.111002.
- Borchert H, Shevchenko EV, Robert A, Mekis I, Kornowski A, Grubel G, Weller H, 2005. Determination of Nanocrystal Sizes: A Comparison of TEM, SAXS, and XRD Studies of Highly Monodisperse CoPt₃ Particles. *Langmuir*, 21(5):1931–1936. doi: 10.1021/la0477183.
- Bungard R. 1996. Ecological and physiological studies of *Clematis vitaba* L. Doctoral (PhD) Theses Lincoln University. <https://core.ac.uk/download/pdf/35461632.pdf>.
- Calabrese EJ, Baldwin LA. 2002. Defining hormesis. *Hum Exp Toxicol.* 21:91–97. doi: 1191/0960327102ht2170a.
- Chhatre A, Solasa P, Sakle S, Thaokar R, Mehra A. 2012. Color and surface plasmon effects in nanoparticle systems: Case of silver nanoparticles prepared by microemulsion route. *Colloids Surf. A Physicochem Eng Asp.* 404:83-92. doi: 10.1016/j.colsurfa.2012.04.016.
- Cui D, Zhang P, Ma Y, He X, Li Y, Zhao Y, Zhang Z. 2014. Phytotoxicity of silver nanoparticles to cucumber (*Cucumis sativus*) and wheat (*Triticum aestivum*). *J Zhejiang Univ Sci A* 15:662–670. doi: 10.1631/jzus.A1400114.
- Da-Cheng H. 2019. Mining chemodiversity from biodiversity: Pharmacophylogeny of Ranunculaceae medicinal plants, In: Da-Cheng H, editor. *Ranunculales medicinal plants*. Academic Press, p. 35-71.
- De Keijzer J, Mulder BM, Janson ME. 2014. Microtubule networks for plant cell division. *Syst Synth Biol.* 8:187–194. doi: 10.1007/s11693-014-9142-x.
- De Ronde JA, van der Mescht A. 1997. 2,3,5-triphenyltetrazolium chloride reduction as a measure of drought tolerance and heat tolerance in cotton. *S Afr J Sci.* 93:431–439.
- Desai R, Mankad V, Gupta SK, Jha P. 2012. Size distribution of silver nanoparticles: UV-visible spectroscopic assessment. *Nanosci Nanotechnol Lett.* 4:30–34. doi: 10.1166/nnl.2012.1278.
- Duke JA. 1985. *CRC Handbook of medicinal herbs*, CRC Press, Boca Raton, Florida.
- El-Ghamery AA, Al-Nahas AI, Mansour MM. 2000. The action of atrazine herbicide as an inhibitor of cell division on chromosomes and nucleic acids content in root meristems of *Allium cepa* and *Vicia faba*. *Cytologia* 65:277-287. doi: 10.1508/cytologia.65.277.
- Eswaran A, Muthukrishnan S, Mathaiyan M, Pradeepkumar S, Rani MK, Manogaran P. 2021. Green synthesis, characterization and hepatoprotective activity of silver nanoparticles synthesized from pre-formulated Liv-Pro-08 poly-herbal formulation. *Appl Nanosci.* doi: 10.1007/s13204-021-01945-x.
- Filippin L, Jović J, Cvrković T, Forte V, Clair D, Toševski I, Boudon-Padieu E, Borgo M., Angelini E. 2009. Molecular characteristics of phytoplasmas associated with flavescence dorée in clematis and grape-

- vine and preliminary results on the role of *Dictyophara europaea* as a vector. *Plant Pathol.* 58:826-837. doi:10.1111/j.1365-3059.2009.02092.x.
- Fiskesjö G. 1985. The *Allium* test as a standard in environmental monitoring. *Hereditas* 102:99-112. doi: 10.1111/j.1601-5223.1985.tb00471.x.
- Geisler-Lee J, Brooks M, Gerfen JR, Wang Q, Fotis C, Sparer A, Ma X, Berg RH, Geisler M. 2014. Reproductive toxicity and life history study of silver nanoparticle effect, uptake and transport in *Arabidopsis thaliana*. *Nanomaterials (Basel)* 4:301-318. doi: 10.3390/nano4020301.
- Geisler-Lee J, Wang Q, Yao Y, Zhang W, Geisler M, Li K, Huang Y, Chen Y, Kolmakov A, Ma X. 2013. Phytotoxicity, accumulation and transport of silver nanoparticles by *Arabidopsis thaliana*. *Nanotoxicology* 7:323-37. doi: 10.3390/nano4020301.
- Gorczyca A, Pocięcha E, Maciejewska-Prończuk J, Kula-Maximenko M, Oćwieja M. 2022. Phytotoxicity of silver nanoparticles and silver ions toward common wheat. *Surf Innov.* 10(1):48-58. doi: 10.1680/jsuin.20.00094.
- Günthardt BF, Hollender J, Hungerbühler K, Scheringer M, Bucheli TD. 2018. Comprehensive toxic plants-phytotoxins database and its application in assessing aquatic micropollution potential. *J Agric Food Chem.* 66:7577-7588. doi: 10.1021/acs.jafc.8b01639.
- Halder NC, Wagner CNJ. 1966. Separation of particle size and lattice strain in integral breadth measurements. *Acta. Cryst.* 20: 312-313. doi: 10.1107/S0365110X66000628.
- Hammann A, Ybanez LM, Isla MI. 2020. Potential agricultural use of a sub-product (olive cake) from olive oil industries composting with soil. *J Pharm Pharmacogn Res.* 8:43-52. doi: 10.56499/jppres19.632_8.1.43.
- Hao DC, He CN, Shen J, Xiao PG. 2017. Anticancer chemodiversity of ranunculaceae medicinal plants: Molecular mechanisms and functions. *Curr Genomics* 18:39-59. doi: 10.2174/1389202917666160803151752.
- Hassan SWM, El-latif HHA. 2018. Characterization and applications of the biosynthesized silver nanoparticles by marine *Pseudomonas* sp. H64. *J Pure Appl Microbiol.* 12:1289-1299. doi: 10.22207/JPAM.12.3.31.
- He J, Lyu RD, Yao M, Xie L, Yang ZZ. 2019. *Clematis mae* (Ranunculaceae), a new species of C. sect. *Meclatis* from Xinjiang, China. *PhytoKeys* 117:133-142. doi: 10.3897/phytokeys.114.31854.
- Heikal Y, Şuğan NA. 2021. Mechanisms of genotoxicity and oxidative stress induced by engineered nanoparticles in plants. In: Khan Z, Ansari MY, Shahwar D (eds) *Induced genotoxicity and oxidative stress in plants*, Springer, Singapore, p. 151-197.
- Hill RL, Wittenburg R, Gourlay AH. 2001. Biology and host range of *Phytophthora vitalbae* and its establishment for the biological control of *Clematis vitalba* in New Zealand. *Biocontrol Sci Technol.* 11:459-473. doi: 10.1080/09583150120067490.
- IBM Corp. Released 2011. IBM SPSS Statistics for Windows, Version 20.0. Armonk, NY: IBM Corp.
- Jacob JM, John MS, Jacob A, Abitha P, Kumar SS, Rajan R, Natarajan S, Pugazhendhi A. 2019. Bactericidal coating of paper towels via sustainable biosynthesis of silver nanoparticles using *Ocimum sanctum* leaf extract. *Mater Res Express.* 6:045401. doi: 10.1088/2053-1591/aafaed.
- Kambale EK, Nkanga CI, Mutonkole BPI, Bapolisi AM, Tassa DO, Liesse JM, Krause AWM, Memvanga PB. 2020. Green synthesis of antimicrobial silver nanoparticles using aqueous leaf extracts from three Congolese plant species (*Brillantaisia patula*, *Crossopteryx febrifuga* and *Senna siamea*). *Heliyon* 6:e04493. doi: 10.1016/j.heliyon.2020.e04493.
- Kaur I, Ellis LJ, Romer I, Tantra R, Carriere M, Allard S, Mayne-L'Hermite M, Minelli C, Unger W, Potthoff A, et al. 2017. Dispersion of nanomaterials in aqueous media: Towards protocol optimization. *J Vis Exp.* 130:e56074. doi: 10.3791/56074.
- Kim KW, Lee DG. 2007. Screening of herbicidal and fungicidal activities from resource plants in Korea. *Korean J Weed Sci.* 27(3):285-295.
- Kthiri A, Hamimed S, Othmani A. 2021. Novel static magnetic field effects on green chemistry biosynthesis of silver nanoparticles in *Saccharomyces cerevisiae*. *Sci Rep.* 11:20078. doi: 10.1038/s41598-021-99487-3.
- Kumar V, Singh DK, Mohan S, Hasan SH. 2016. Photo-induced biosynthesis of silver nanoparticles using aqueous extract of *Erigeron bonariensis* and its catalytic activity against acridine orange. *J Photochem Photobiol B: Biol.* 155:39-50. doi: 10.1016/j.jphoto-biol.2015.12.011.
- Lalsangpuii F, Rokhum SL, Nghakliana F, Fakawmi L, Ruatpuia JVL, Laltlanmawii E, Lalfakzuala R, Siana Z. 2022. Green Synthesis of Silver Nanoparticles Using *Spilanthes acmella* Leaf Extract and its Antioxidant-Mediated Ameliorative Activity against Doxorubicin-Induced Toxicity in Dalton's Lymphoma Ascites (DLA)-Bearing Mice. *ACS Omega.* 7(48):44346-44359. doi: 10.1021/acsomega.2c05970.
- Lang I, Sassmann S, Schmidt B, Komis G. 2014. Plasmolysis: Loss of turgor and beyond. *Plants* 3:583-59. doi: 10.3390/plants3040583.
- Łaska G, Maciejewska-Turska M, Sieniawska E, Świątek Ł, Pasco DS, Balachandran P. 2021. Extracts from

- Pulsatilla patens* target cancer-related signaling pathways in HeLa cells. *Sci Rep.* 11(1):10654. doi: 10.1038/s41598-021-90136-3.
- Lewis SN, Balick MJ. 2020. Handbook of poisonous and injurious plants. New York Botanical Garden, Spinger, New York, U.S.A
- Marichal L, Klein G, Armengaud J. 2020. Protein corona composition of silica nanoparticles in complex media: Nanoparticle size does not matter. *Nanomaterials* 10:240. doi: 10.3390/nano10020240.
- Martínez-Castañón GA, Niño-Martínez N, Martínez-Gutierrez F. 2008. Synthesis and antibacterial activity of silver nanoparticles with different sizes. *J Nanopart Res.* 10:1343–1348. doi: 10.1007/s11051-008-9428-6.
- Monopoli MP, Aberg C, Salvati A, Dawson KA. 2012. Biomolecular coronas provide the biological identity of nanosized materials. *Nat Nanotechnol.* 7:779–786. doi: 10.1038/nnano.2012.207.
- Muala WCB, Desobgp ZSC, Jong NE. 2021. Optimization of extraction conditions of phenolic compounds from *Cymbopogon citratus* and evaluation of phenolics and aroma profiles of extract. *Heliyon* 7:e06744. doi: 10.1016/j.heliyon.2021.e06744.
- Naz I, Ramchandani S, Khan MR, Yang MH, Ahn KS. 2020. Anticancer potential of raddeanin A, a natural triterpenoid isolated from *Anemone raddeana* Regel. *Molecules* 25:1035. doi: 10.3390/molecules25051035.
- Nefic H, Musanovic J, Metovic A, Kurteshi K. 2013. Chromosomal and nuclear alterations in root tip cells of *Allium cepa* L. induced by alprazolam. *Med Arch* 67(6):388–392. doi: 10.5455/medarh.2013.67.388-392.
- O'Halloran W. 2019. Management of *Clematis vitalba* at 'Suez Pond'. Assessment of monitoring and control using manual methods. Wild Eork, SECAD. <https://www.wildwork.ie/wp-content/uploads/2022/01/Management-of-Clematis-vitalba-at-Suez-Pond.pdf>. Accessed 3.10. 2023.
- Ogle CC, Cock GD, Arnold G, Mickleson N. 2000. Impact of an exotic vine *Clematis vitalba* (F. Ranunculaceae) and of control measures on plant biodiversity in indigenous forest, Taihape, New Zealand. *Austral Ecol.* 25:539–551. doi: 10.1046/j.1442-9993.2000.01076.x.
- Panda KK, Achary VMM, Krishnaveni R, Padhi BK, Sarangi SN, Sahu SN, Panda BB. 2011. *In vitro* biosynthesis and genotoxicity bioassay of silver nanoparticles using plants. *Toxicol In Vitro* 25:1097–1105. doi: 10.1016/j.tiv.2011.03.008.
- Piloni A, Wong CK, Chen F, Lord M, Walther A, Stenzel MH. 2019. Surface roughness influences the protein corona formation of glycosylated nanoparticles and alter their cellular uptake. *Nanoscale* 11:23259–23267. doi: 10.1039/C9NR06835J.
- Prajitha V, Thoppil JE. 2017. Cytotoxic and apoptotic activities of extract of *Amaranthus spinosus* L. in *Allium cepa* and human erythrocytes. *Cytotechnology* 69:123–133. doi: 10.1007/s10616-016-0044-5.
- Prakash P, Gnanaprakasam P, Emmanuel R, Arokiyaraj S, Saravanan M. 2013. Green synthesis of silver nanoparticles from leaf extract of *Mimulus elengi* Linn. for enhanced antibacterial activity against multi drug resistant clinical isolates. *Colloids Surf B* 108:255–259. doi: 10.1016/j.colsurfb.2013.03.017.
- Pramanik S, Chatterjee S, Saha A, Devi PS, Kumar GS, 2016. Unraveling the Interaction of Silver Nanoparticles with Mammalian and Bacterial DNA. *J Phys Chem B* 120(24):5313–5324. doi: 10.1021/acs.jpcc.6b01586.
- Rasband WS. 1997–2018. ImageJ, U.S. National Institutes of Health, Bethesda, Maryland, USA, <https://imagej.nih.gov/ij/>.
- Rasmussen CG, Wright AJ, Müller S. 2013. The role of the cytoskeleton and associated proteins in determination of the plant cell division plane. *Plant J.* 75:258–269. doi: 10.1111/tpj.12177.
- Reddy NV, Li H, Hou T. 2021. Phytosynthesis of silver nanoparticles using *Perilla frutescens* leaf extract: Characterization and evaluation of antibacterial, antioxidant, and anticancer activities. *Int J Nanomed.* 16:15–29. doi: 10.2147/IJN.S265003.
- Redmond CM, Stout JC. 2018. Breeding system and polination ecology of a potentially invasive alien *Clematis vitalba* L. in Ireland. *J Plant Ecol.* 11:56–63. doi: 10.1093/jpe/rtw137.
- Riaz Ahmed KB, Nagy AM, Brown RP, Zhang Q, Malghan SG, Goering PL. 2017. Silver nanoparticles: Significance of physicochemical properties and assay interference on the interpretation of *in vitro* cytotoxicity studies. *Toxicol In Vitro* 38:179–192. doi: 10.1016/j.tiv.2016.10.012.
- Roy B, Krishnan SP, Chandrasekaran N, Mukherjee A. 2019. Toxic effects of engineered nanoparticles (metal/metal oxides) on plants using *Allium cepa* as a model system. *Compr Anal Chem.* 84:125–143. doi: 10.1016/bs.coac.2019.04.009.
- Roy P, Das B, Mohanty A, Mohapatra S. 2017. Green synthesis of silver nanoparticles using *Azadirachta indica* leaf extract and its antimicrobial study. *Appl Nanosci.* 7:843–850. doi: 10.1007/s13204-017-0621-8.
- RuttkeyNedecky B, Krystofova O, Nejdil L, Adam V. 2017. Nanoparticles based on essential metals and their phytotoxicity. *J Nanobiotechnol.* 15:33. doi: 10.1186/s12951-017-0268-3.

- Segneanu A-E, Grozescu I, Czipl F, Berki D, Damian D, Niculite CM, Florea A, Leabu M. 2015. *Hel-leborus purpurascens* - Amino acid and peptide analysis linked to the chemical and antiproliferative properties of the extracted compounds. *Molecules* 20:22170–2218. doi: 10.3390/molecules201219819.
- Shende S, Rajput VD, Gade A, Minkina T, Fedorov Y, Sushkova S, Mandzhieva S, Burachevskaya M, Boldyreva V. 2022. Metal-Based Green Synthesized Nanoparticles: Boon for Sustainable Agriculture and Food Security. *IEEE T Nanobiosci.*, 21(1):44-54. doi: 10.1109/TNB.2021.3089773.
- Sutan AN, Vilcoci DS, Fierascu I, Neblea AM, Sutan C, Ducu C, Soare LC, Negrea D, Avramescu SM, Fierascu RC. 2019. Influence of the phytosynthesis of noble metal nanoparticles on the cytotoxic and genotoxic effects of *Aconitum toxicum* Reichenb. leaves alcoholic extract. *J Clust Sci.* 30:647-660. doi: 10.1007/s10876-019-01524-9.
- Șuțan NA, Matei AN, Oprea E, Tecuceanu V, Tătaru LD, Moga SG, Manolescu DS, Topală CM. 2020. Chemical composition, antioxidant and cytogenotoxic effects of *Ligularia sibirica* (L.) Cass. roots and rhizomes extracts. *Caryologia* 73:83-92. doi: 10.13128/caryologia-116.
- Șuțan NA, Fierăscu I, Fierăscu RC, Manolescu DS, Soare CL. 2016. Comparative analytical characterization and *in vitro* cytogenotoxic activity evaluation of *Asplenium scolopendrium* L. leaves and rhizome extracts prior to and after Ag nanoparticles phytosynthesis. *Ind Crops Prod.* 83:379-386. doi: 10.1016/j.indcrop.2016.01.011.
- Șuțan NA, Fierascu I, Șuțan C, Soare LC, Neblea AM, Somoghi R., Fierăscu RC. 2021. *In vitro* mitodepressive activity of phytofabricated silver oxide nanoparticles (Ag₂O-NPs) by leaves extract of *Hel-leborus odoratus* Waldst. & Kit. ex Willd. *Mater Lett.* 286:129194. doi: 10.1016/j.matlet.2020.129194.
- Taurozzi JS, Hackley VA, Wiesner MR. 2011. Ultrasonic dispersion of nanoparticles for environmental, health and safety assessment--issues and recommendations. *Nanotoxicology* 5:711-729. doi: 10.3109/17435390.2010.528846.
- Towill LE, Mazur P. 1975. Studies on reduction of 2,3,5-triphenyltetrazolium chloride as a viability assay for plant tissue cultures. *Can J Bot Revue Can Bot.* 53:1097–1102.
- Tyagi PK, Tyagi S, Gola D, Arya A, Ayatollahi A, Alshehri MM, Sharifi-Rad J. 2021. Ascorbic acid and polyphenols mediated green synthesis of silver nanoparticles from *Tagetes erecta* L. aqueous leaf extract and studied their antioxidant properties. *J Nanomater.* 6515419. doi: 10.1155/2021/6515419.
- Valencia-Avilés E, García-Pérez ME, Garnica-Romo MG, Figueroa-Cárdenas JDD, Meléndez-Herrera E, Salgado-Garciglia R, Martínez-Flores HE. 2018. Antioxidant properties of polyphenolic extracts from *Quercus laurina*, *Quercus crassifolia*, and *Quercus scytophylla* Bark. *Antioxidants* 7:81. doi:10.3390/antiox7070081.
- Valster AH, Hepler PK. 1997. Caffeine inhibition of cytokinesis: effect on the phragmoplast cytoskeleton in living *Tradescantia* stamen hair cells. *Protoplasma* 196:155–166. doi: 10.1007/BF01279564.
- Vijayaraghavareddy P, Adhinarayanreddy V, Vemanna RS, Sreeman S, Makarla U. 2017. Quantification of membrane damage/cell death using Evan's blue staining technique. *Bio Protoc.* 7:1-8. doi: 10.21769/BioProtoc.2519.
- Weng-Tsai W. 2003. A revision of *Clematis* sect. *Clematis* (Ranunculaceae). *J Syst Evol* 41:1-62
- Wieczerek M, Namieśnik J, Kudłak B (2016) Bioassays as one of the green chemistry tools for assessing environmental quality: A review. *Environ Int.* 94:341-361. doi: 10.1016/j.envint.2016.05.017.
- Wink M. 2010. Mode of action and toxicology of plant toxins and poisonous plants. *Julius Kühn Archiv.* 93-112.
- Woudenberg JH, Aveskamp MM, de Gruyter J, Spiers AG, Crous PW. 2009. Multiple *Didymella* teleomorphs are linked to the *Phoma clematidina* morphotype. *Persoonia* 22:56–62. doi: 10.3767/003158509X427808.
- Wypij M, Jędrzejewski T, Trzcińska-Wencel J, Ostrowski M, Rai M, Golińska P. 2021. Green synthesized silver nanoparticles: Antibacterial and anticancer activities, biocompatibility, and analyses of surface-attached proteins. *Front Microbiol.* 12:632505. doi: 10.3389/fmicb.2021.632505.
- Yan A, Chen Z. 2019. Impacts of silver nanoparticles on plants: A focus on the phytotoxicity and underlying mechanism. *Int J Mol Sci.* 20:1003. doi: 10.3390/ijms20051003.